Journal of Biomolecular NMR, **12:** 243–257, 1998.
KLUWER/ESCOM

Nuclear magnetic resonance characterization of a paramagnetic DNA-drug complex with high spin cobalt; assignment of the ^{1}H and ^{31}P NMR spectra, and determination of electronic, spectroscopic and molecular properties

Miriam Gochin
Department of Microbiology, University of the Pacific School of Dentistry, CA 94115 and Department of Pharmaceutical Chemistry, University of California, San Francisco, CA 94143, U.S.A.

Received 6 January 1998; Accepted 23 March 1998

Key words: DNA, chromomycin, cobalt, paramagnetic, hyperfine shift, paramagnetic relaxation, susceptibility

Abstract

The proton NMR spectrum of the ternary complex between the octamer duplex d(TTGGCCAA)$_2$, two molecules of the drug chromomycin-A$_3$, and a divalent cobalt ion has been assigned. Assignment procedures used standard two-dimensional techniques and relied upon the expected NOE contacts observed in the equivalent diamagnetic complex containing zinc. The magnetic susceptibility tensor for the cobalt was determined and used to calculate shifts for all nuclei, aiding in the assignment process and verification. Relaxation, susceptibility, temperature and field dependence studies of the paramagnetic spectrum enabled determination of electronic properties of the octahedral cobalt complex. The electronic relaxation rate τ_s was determined to be 2.5 $\pm$ 1.5 ps; the effective isotropic *g* value was found to be 2.6 $\pm$ 0.2, indicating strong spin-orbit coupling. The magnetic susceptibility tensor was determined to be $\chi_{xx} = 8.9 * 10^{-3}$ cm^3/mol, $\chi_{yy} = 9.5 * 10^{-3}$ cm^3/mol, χ_{zz} = 12.8 $* 10^{-3}$ cm^3/mol. A tentative rotational correlation time of 8 ns was obtained for the complex. Both macroscopic and microscopic susceptibility measurements revealed deviations from Curie behavior over the temperature range accessible in the study. Non-selective relaxation rates were found to be inaccurate for defining distances from the metal center. However, pseudocontact shifts could be calculated with high accuracy using the dipolar shift equation. Isotropic hyperfine shifts were factored into contact and dipolar terms, revealing that the dipolar shift predominates and that contact shifts are relatively small.

Introduction

Much of the literature on NMR studies of paramagnetic biomolecules has involved the study of metalloproteins containing iron, such as heme proteins and FeS cluster proteins (for reviews, see Cheng and Markley, 1995; Bertini and Luchinat, 1986; Marion, 1994; Bertini et al., 1996a). Many of the studies have been aimed at investigation of the electron distribution around the active site as a probe of electron transfer and structure–function relationships (La Mar et al., 1973). There are a number of examples investigating Co(II) in various heme proteins and in proteins such as cobalt-substituted carbonic anhydrase (Bertini et al., 1994) , superoxide dismutase (Sette et al., 1993; Renault et al., 1997), blue copper proteins (Vila and Fernandez, 1996) and a cobalt-substituted zinc finger (Harper et al., 1993) . This work describes the first detailed analysis of a cobalt complex involving DNA.

Recently a number of authors have demonstrated the feasibility of including the paramagnetic shifts as constraints in structure determination (Gochin and Roder, 1995; Banci et al., 1997a,b; Salgueiro et al., 1997) For the majority of protons in a large metallo-biopolymer, the paramagnetic shift is composed entirely of the pseudocontact (isotropic dipolar) term, since the contact term is restricted to groups ligated around the metal. The pseudocontact term is

directly related to the geometry of the protons in the principal axis system of the electronic susceptibility tensor (Bertini and Luchinat, 1986). The pseudocontact shift is of particular interest as a long-range constraint to improve upon the quality of structures of molecules that have extended linear domains, regions of limited secondary structure or multiple domains. This includes DNA, RNA and their complexes, and loops of proteins, where NOE contacts are sparse. We have chosen to study a DNA complex with a drug and divalent cobalt, to demonstrate the scope and potential of the pseudocontact shifts in defining structure (Gochin, 1997) . The octamer duplex $d(TTGGCCAA)_2$ forms a tightly bound ternary complex with chromomycin-A_3 and several divalent metals (Gao and Patel, 1990). Chromomycin-A_3 consists of a partially aromatic chromophore to which a hydrophilic side chain, a disaccharide segment (A-B) and a trisaccharide segment (C-D-E) are attached (structure **I**). It binds to a GC step in DNA with a stoichiometry of two drug molecules per DNA duplex. A single divalent metal ion binds tightly to the O1 and O9 oxygen atoms of the two chromophores. For our purposes, the isostructural complexes formed with Co^{2+} and Zn^{2+} are used, since these two ions have identical ionic radii. The paramagnetic shift is defined as the difference between the shifts observed for the cobalt (paramagnetic) and zinc (diamagnetic) structures. The NMR structure of a Mg^{2+} complex with the similar duplex $d(AAGGCCTT)_2$ has been published (Gao et al., 1992)

The NMR spectrum of the DNA–drug–Co^{2+} complex and of paramagnetic macromolecules in general, is complicated by line broadening and non-standard chemical shifts. It is not immediately apparent that the spectrum can be assigned using standard procedures. Here we describe the assignment of the proton and phosphorus NMR spectrum of the cobalt (and zinc) complexes, obtain various parameters of the complex, such as correlation times τ_c (molecular) and τ_r (rotational), measure the solution magnetic anisotropy, derive the magnetic susceptibility tensor and determine the contact shift contributions. We show that the pseudocontact shifts predominate and can be calculated accurately assuming metal-centered shifts alone. In addition to probing the electronic properties of the complex, the results demonstrate that octahedrally coordinated cobalt is suitable for use in NMR as a structural tool.

Experimental Methods

Sample preparation

DNA was purchased from Oligo's Etc; cobalt chloride from Sigma, and chromomycin-A_3 from Calbiochem. The complex between $d(TTGGCCAA)_2$, cobalt and chromomycin was formed by adding a stoichiometric amount of chromomycin (2:1) to a solution containing either 4.5 mM or 2 mm duplex DNA and 4.5 mM or 2 mM $CoCl_2$ in D_2O buffer (100 mM NaCl, 10 mM sodium borate, pH 8.1). The concentration of the DNA was determined by measuring the extinction coefficient (Griswold, et al., 1951) which was found to be 120 900 $m^{-1}cm^{-1}$ at 260 nm. Chromomycin was dissolved into a dilute aqueous solution, and the concentration was determined from the extinction coefficient, $E_{405} = 8800\ m^{-1}\ cm^{-1}$ in 100 mM sodium borate, 200 mM NaCl at pH 8 (Banville et al., 1990). It was then lyophilized and concentrated several times from D_2O to ensure ease of dissolution when added in solid form to the sample. The pH of the final sample was adjusted to 5.9. A similar complex with zinc was formed using 2 mM duplex DNA, yielding a final solution at pH 5.6, and with magnesium, forming a 1.5 mM solution of the complex at pH 5.8. Samples of the cobalt and zinc complexes were also prepared in 90% H_2O, 10% D_2O.

The correct stoichiometry of complex formation was ensured by following the peaks in a ^{31}P spectrum, which were very sensitive to the presence of uncomplexed metal ion.

NMR Experiments

NMR experiments were performed on a GE Omega system at 500 MHz. Varying field experiments were also conducted on a QE 300 and a Varian 600 MHz machine. One-dimensional ^1H and ^{31}P spectra were recorded at three field strengths and temperatures varying from 20–45 °C. One-dimensional spectra of the cobalt sample in H_2O were recorded using either presaturation or the WATERGATE sequence (Piotto et al., 1992) for water suppression. Two dimensional double quantum-filtered COSY (DQFCOSY) and NOESY experiments were recorded at 500 MHz, two temperatures, 25 °C and 35 °C, and two pH s (for the Co sample) pH 3.5 and pH 5.9. The 1024×2048 DQFCOSY and NOESY spectra of the zinc complex were recorded with 16 scans per FID and a spectral width of 5000 Hz. The double quantum-filtered COSY spectrum of the cobalt complex was recorded with

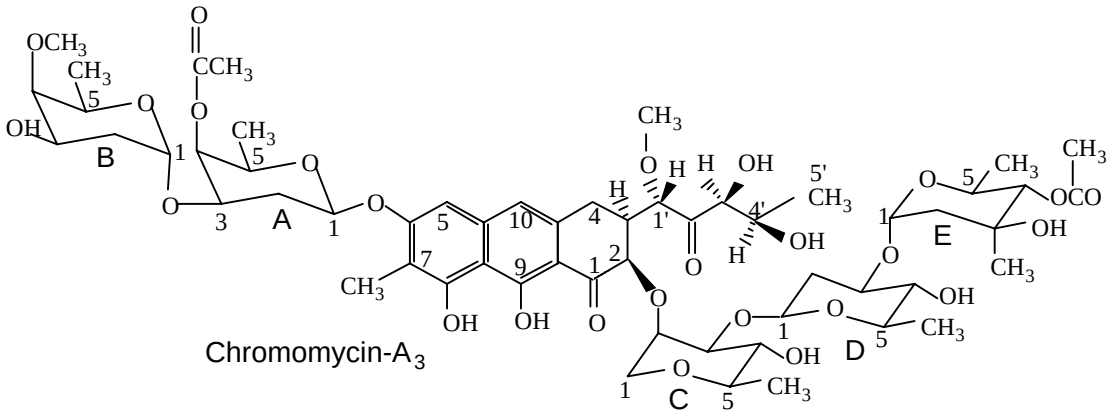

Structure I.

spectral width 12 kHz, digital resolution 6 Hz/pt in ω_2, collecting 2048 FID's of 32 scans each. The two-dimensional NOE spectrum of the cobalt complex was recorded with a 200 ms mixing time, spectral width 20 kHz, digital resolution 10 Hz/pt in ω_2, collecting 2048 FID's of 32 scans each. Residual HDO was suppressed with the T_1-null condition. For NOE spectra recorded in 90% H_2O, presaturation followed by a SCUBA delay (Brown et al., 1988) was used to suppress solvent. Two dimensional TOCSY spectra of the cobalt complex were recorded with an MLEV-16 multipulse train (Levitt et al., 1982) of 30 ms or 65 ms with 1 ms trim pulses, using the same spectral parameters as for the DQFCOSY experiment. A SCUBA delay was used to suppress residual HDO. A two-dimensional $^{31}P - {}^{1}H$ spectrum was recorded for the Zn complex (Sklenar et al., 1986) The one dimensional proton spectrum and 1D NOE's of the cobalt complex were recorded with a spectral width of 70 kHz (140 ppm at 500 MHz). Irradiation times of 0.1 s–0.4 s and irradiation strengths 50 to 100 Hz were used for the 1D NOE experiments. ^{31}P shifts were references to external trimethyl phosphate (TMP) and ^{1}H shifts to external trimethyl silyl pentanoic acid (TSP). The external references were placed in capillary tubes inserted into the center of the NMR tubes. Paramagnetic longitudinal relaxation was determined by non-selective inversion recovery experiments, which were fit with mono-exponential decay curves. The T_{1M} was measured for protons that gave well-dispersed signals in 1D spectra of both the Co(II) and Zn(II) complexes, by taking the difference of the $T_1{}^{-1}$ rates in the two complexes. T_{2M} was measured for every proton from the difference in linewidths in 1D spectra or 2D NOESY plots of the Co(II) and Zn(II) complexes.

The isotropic susceptibility of the solution was measured from the shift difference δ_{TSP} between the TSP reference dissolved in the sample and an external TSP reference in the same buffer in a coaxial capillary. Susceptibility of equal concentrations of both the diamagnetic and paramagnetic complexes were measured. The paramagnetic component of the TSP shift was determined as $\Delta_{TSP} = \delta_{TSP}(\mathrm{Co}) - \delta_{TSP}(\mathrm{Zn})$.

One- dimensional data were processed using Felix software (Biosym Technologies, San Diego, CA). Two-dimensional spectra were processed using STRIKER (Day, 1994) and analyzed using SPARKY 3.0 (Goddard and Kneller, 1997).

Simulations

The paramagnetic shift is defined as the difference in observed shifts between the two complexes:

$$\delta_{obs}(\mathrm{ppm}) = \delta_{para} + \delta_{dia} = \delta_{dip} + \delta_{con} + \delta_{dia} \quad (1)$$

where δ_{dia} is the observed shift in the zinc complex, and δ_{para} the paramagnetic component of the observed shift in the cobalt complex, δ_{obs}. δ_{para} may contain components δ_{dip} and δ_{con} for the pseudocontact and contact terms, respectively. The magnetic susceptibility tensor χ was determined by minimizing the difference between a set of observed paramagnetic shifts and those calculated either from the PDB coordinates for the similar complex with $d[AAGGCCTT]_2$ and Mg^{2+} (Gao et al., 1992) or from our refined structure (Tu and Gochin, in preparation). The variables adjusted were the magnetic susceptibility tensor anisotropy magnitudes $\Delta\chi_{ax}$ and $\Delta\chi_{rh}$ and the three Euler angles defining the orientation of χ with respect to the molecular reference frame, according to the equation:

$$\delta_{dip}(ppm) = \frac{1}{3r^3} \left\{ \Delta\chi_{ax}(3\cos^2\theta - 1) + \frac{3}{2}\Delta\chi_{rh}\sin^2\theta\cos 2\phi \right\} \quad (2)$$

where (r,θ,ϕ) are the spherical coordinates of the observed nucleus in the principal axis system of the susceptibility tensor. Powell minimization was used (Press et al., 1992) to minimize the mean square difference between observed and calculated pseudocontact shifts.

Molecular graphics images were created using the MIDASPLUS program from the Computer Graphics Laboratory at UCSF (Ferrin et al., 1988) .

Results

To determine the experimental pseudocontact shift and hence the susceptibility tensor, spectra of the paramagnetic and an analogous diamagnetic complex must be assigned (Equation 1). It is necessary that the two complexes be structurally identical in order to avoid diamagnetic shift changes which cannot be accurately calculated. To this end, the spectra of two diamagnetic complexes were compared to verify that no structural changes occurred upon substitution of different metal ions.

Spectra of the Zinc and Magnesium Complexes

The spectra of these complexes proved trivial to assign, since the assignment had already been described for the Mg^{2+} complex (Gao and Patel, 1989). The deoxyribose H5′ and H5″ resonances which were not assigned earlier have been assigned in this study. Observed ^{1}H chemical shifts in the Mg^{2+} complex were found to differ from those described by Gao and Patel, by 0.07–0.11 ppm. These differences occurred principally in the DNA resonances and are assumed to arise from the different pH used in that study. Minimal differences occurred between the chemical shifts of the zinc and magnesium complexes in D_2O, all lying within the error of measurement in the two-dimensional spectra (i.e. $<$0.03 ppm: This value is calculated from the experimental error in measuring the difference of two observed shifts at the digital resolution specified in Experimental Methods), with the exception of the G4H1' proton (0.05 ppm difference), and the chromomycin methyl H7 group (0.04 ppm difference). These protons all lie very close to the site of complexation, and differences in the ionic radii or electronic structure of the metal ions could account for the observed effects. These must be taken into account when establishing the paramagnetic component of the shift.

Observed ^{31}P chemical shifts were identical for the zinc and magnesium complexes, although these differed substantially both in sign and magnitude from those reported earlier (Gao and Patel, 1989) , using the same reference (TMP). The reason for this discrepancy is not known. The spectra look qualitatively identical. In addition, analysis of a two-dimensional heteronuclear ^{31}P – ^{1}H correlation spectrum of the zinc complex resulted in a switch of the assignments of the P(G4-C5) and P(C6-A7) resonances compared to the earlier study.

Spectra of the Cobalt complex

The one-dimensional proton spectrum of the cobalt complex at 25 °C is shown in Figure 1. Resonances are observed between +42 and −60 ppm in the ^{1}H spectrum. All resonances shifted out of the main envelope (0–10 ppm) show a strong temperature dependence, which is linear over the range 15–40 °C. Evidence of a quadratic component is observed by extrapolating back to the diamagnetic shift (at $1/T = 0$ K^{-1}). Examples of this effect are shown in Figure 2 for the chromophore protons which are subject to both contact and pseudocontact shifts, although a very similar result is observed for the strictly pseudocontact-shifted protons (eg. DNA protons). The extrapolated lines of the observed δ_{para} do not pass through the origin at $1/T = 0$. This behavior indicates deviations of the pseudocontact shift from Curie behavior due to the anisotropy of the *g*-tensor and/or the presence of sizeable zero field splitting at the cobalt (Kurland and McGarvey, 1970) . The Curie slope of the hyperfine shift over the 15–40 °C range is directly proportional to the size of the shift, indicating that deviations from Curie behavior cannot be detected over this small temperature range (Emerson and La Mar, 1990). In addition, because most protons experience only pseudocontact shifts, without a contact contribution, the proportionality of Curie slope to shift size is an indication that the structure of the complex is remaining invariant over the temperature range studied.

Line broadening effects due to the Co^{2+} ion range from $<$5 Hz for protons more than $\approx$ 18 Å from the metal to several hundred Hz for protons within a 5 Å radius of the metal. Apart from the protons of the chromophore which experience contact shifts and re-

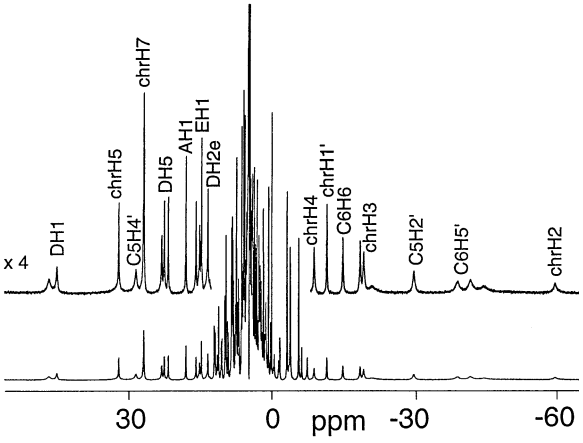

Figure 1. One-dimensional ^{1}H spectrum of 2 mM d(TTGGCCAA)$_2$ bound to two equivalents of chromomycin and one equivalent of Co(II) at 25 °C and 500 MHz. 128 scans were recorded with an acquisition delay of 1s and a spectral width of 80 kHz.

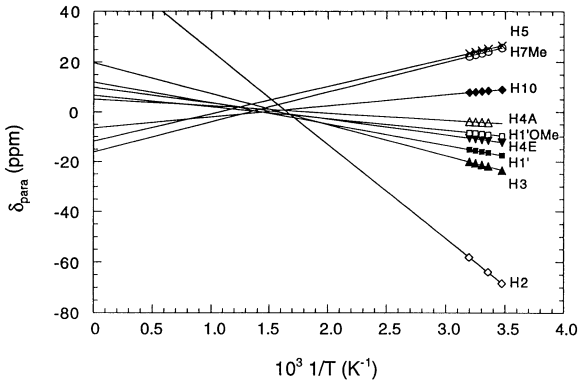

Figure 2. Plot of the paramagnetic component δ_{para} (Equation 1) of the chemical shift of chromomycin chromophore protons as a function of the inverse temperature. The data were extrapolated linearly to $T^{-1} = 0$ K.

laxation effects, the primary relaxation mechanism is due to Curie rather than dipolar broadening.

The 1D ^{31}P spectrum is shown in Figure 3. Drug complexation causes some increased dispersion of the ^{31}P resonances in the diamagnetic complex compared to free DNA, due to perturbation at the site of complexation. In the Co^{2+} complex, large long-range ^{31}P pseudocontact shifts occur, with virtually no increase in the linewidths. The most upfield shifted phosphate, at −14.2 ppm could be identified as P(C5–C6) because of its proximity to the metal ion.

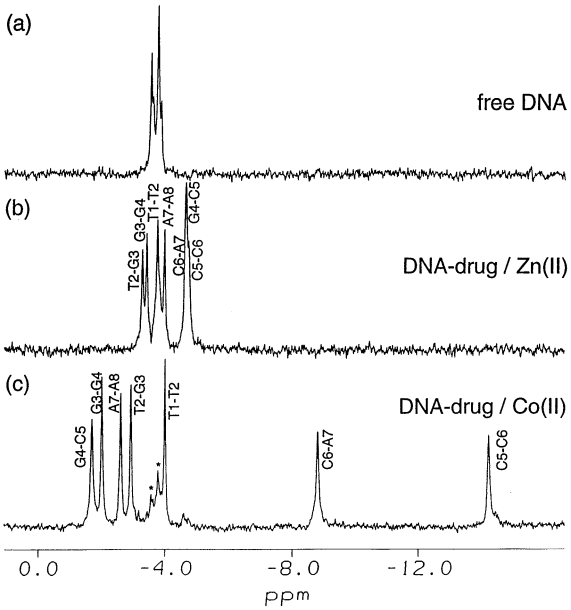

Figure 3. ^{31}P spectra of the DNA at 25 °C and 500 MHz. (a) Free DNA, 32 scans; (b) DNA–chromomycin–Zn(II) complex, 128 scans; (c) DNA–chromomycin–Co(II) complex, 128 scans. An acquisition delay of 2 s and spectral width of 5000 Hz were used. Spectra were referenced to external TMP. 3 Hz line broadening was applied.

Assignment of non-exchangeable protons in the Co^{2+} spectrum

Four methyl groups shifted upfield out of the main proton envelope were immediately recognized by their relative intensities in the 1D ^{1}H spectrum. Sequence specific resonance assignments started with the observation of an NOE correlation between two of these methyl groups, enabling identification of these methyls as C(H6) and chr(OMe). The observed NOE connectivities around these residues then led to assignment of the aliphatic side chain of the chromomycin chromophore, as well as the H4 proton of the C-sugar.

The C-sugar and P(C5–C6) chemical shifts were used to derive a starting value for the magnetic susceptibility tensor from the existing structure (Gao et al., 1992). Because of the C2 axis of symmetry of this complex, three shifts are sufficient to determine the five parameters of the tensor. The set of calculated shifts for the remaining protons and phosphates could then be used for validating further assignments.

Assignment proceeded by using standard COSY and NOESY two-dimensional spectroscopy for the protons between −12 and +18 ppm, and one-dimensional NOEs for the far-shifted resonances. No further NOE connectivities could be traced from the

protons identified on the C-sugar, presumably due to broadening of the C-sugar H1, H2, H3 and H5 resonances. We were able to identify a strong NOESY and COSY cross-peak at (3.21,7.23 ppm) as belonging to the B-sugar methyl-H5 interaction. All of the residues of the B-sugar were then assigned from the COSY and NOESY correlations. A remarkably good agreement with the calculated B-sugar protons was found, with an RMS deviation of 0.2 ppm over an observed paramagnetic shift range of 1–3.3 ppm.

NOE connectivities between the various chromomycin sugars as well as between sugars A, B, D and E to DNA protons were used to complete sequence specific assignments. Overlapped peaks were resolved by looking at spectra at higher temperature, at which protons sharpened and shifted; this was particularly useful for the G4 spin system. Varying pH and temperature also enabled resolution of the otherwise overlapped G3H1′, BH1 and A7H1′ resonances.

The spectra in Figure 4 demonstrate the chemical shift dispersion, the quality of the NOESY spectra, as well as the extent to which regular DQFCOSY cross-peaks may be observed. About 60% of the expected cross-peaks are observed in the DQFCOSY spectrum, the closest pair of protons observed is the G4H2′-2″ cross-peak, which are 7.7 and 7.8 Å from the cobalt. Apart from that cross-peak, which has a large geminal coupling constant, protons closer than about 10 Å do not give DQFCOSY cross-peaks. In addition, an example is shown in Figure 4 of a cross-correlation cross-relaxation induced DQFCOSY cross peak (Wimperes and Bodenhausen, 1989; Bertini et al., 1993) between AH3 and BH1, which are not scalar coupled. These spurious cross-peaks could be identified because they do not appear in the corresponding TOCSY spectrum (Desvaux and Gochin, in preparation). A total of four of these relaxation-allowed cross-peaks occurred in the entire DQFCOSY spectrum.

The protons of DNA residues C5 and C6 as well as those of the chromophore of the chromomycin, are dramatically shifted and occur mostly outside the main envelope of the spectrum from 0–12 ppm. They were assigned by 1D NOE methods. Figure 5a shows an example of irradiation of the C5H2′ proton at −29.51 ppm (4.8 Å from Co^{2+}) and the presence of strong NOEs to C6H6 as well as to C6H5 and C5H3′. The geminal proton C5H2″ is ≈ 4 Å from the Co^{2+} and was identified as a peak with 500 Hz linewidth at −20.84 ppm. Irradiation of this peak in Figure 5b shows an NOE connectivity to the C5H2' proton. The rapid relaxation of the C5H2″ proton competes with the polarization transfer so that no NOE transfer from C6H2′ to C6H2″ is observed in Figure 5a and a very small H2″–H2′ NOE is seen in Figure 5b. Thus the 1D NOE can often be observed from a broader to a narrower resonance but not *vice versa*. Nevertheless, the presence of significant paramagnetic relaxation does not preclude the observation of NOEs in this complex nor their use for assignment purposes. A figure showing the 1D NOE assignments of the chromophore protons is available as supplementary material.

Assignment of exchangeable protons in the Co^{2+} spectrum

Exchangeable DNA base protons of the central four base pairs G3–G6 were observed and assigned by standard procedures. The exchangeable base protons of T1, T2, A7 and A8 were exchanging too rapidly at 25 °C to be observed. A peak at 14.63 ppm, which is present with either presaturation or watergate suppression of the H_2O, has been assigned to the slowly exchanging hydroxyl proton of the D sugar. The chromophore OH8 proton was not located – it is expected to be shifted by more than 100 ppm (see below).

Assignment of the ^{31}P spectrum

The phosphorus resonances were assigned mainly by comparison of observed and calculated chemical shifts relative to the zinc complex, and also by using the observed line broadening effect and its dependence on distance from the metal center.

The proton chemical shifts of the cobalt complex of $d(TTGGCCAA)_2$ and chromomycin-A_3 are listed in Table 1. A table of zinc assignments and the ^{31}P chemical shifts for both the cobalt and zinc complexes are available as Supplementary Material. All chemical shifts have also been deposited with the Biomagnetic Resonance Data Bank.

Electronic properties at the metal site

The electronic relaxation time, isotropic *g* value and susceptibility tensor were determined from analysis of the NMR spectra.

Susceptibility measurements

The solution magnetic moment of the cobalt complex was measured from the isotropic shift of the inert TSP reference relative to that in the zinc complex (see Experimental Methods). A value of 0.073 ppm for the isotropic shift Δ_{TSP}(Co–Zn) was obtained at 25 °C for

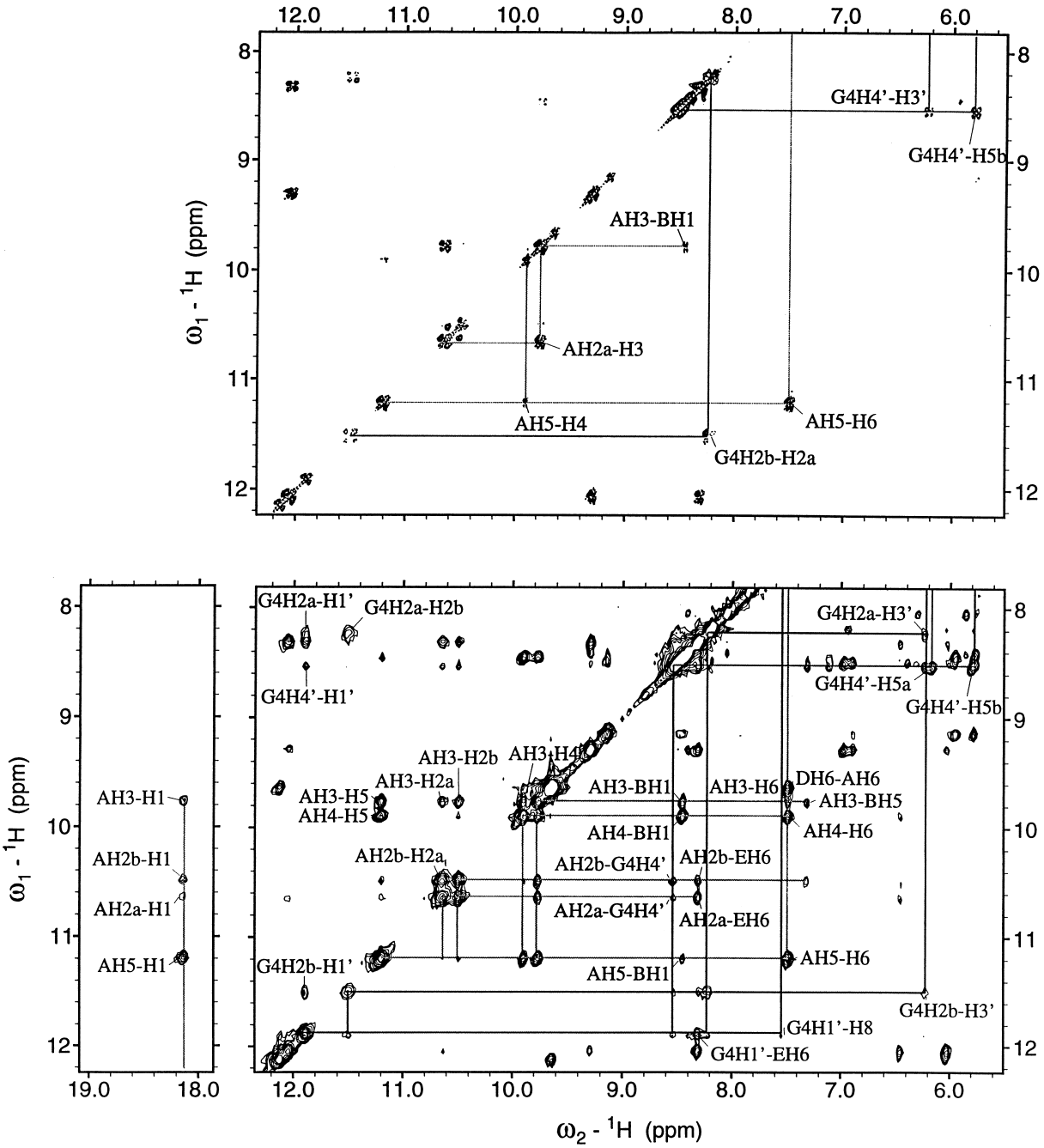

Figure 4. Two-dimensional DQFCOSY (top) and 200 ms NOESY (bottom) plots of the chromomycin A sugar and DNA G4 residue in the Co(II) complex. Peaks in the DQFCOSY spectrum are limited to those which do not show excessive broadening due to the Co(II) relative to *J*-coupling values. G4 sugar protons range from 8 to 12 Å from the Co(II). A DQFCOSY peak between the non-*J*-coupled pair AH3 and BH1 is indicated. In the NOESY spectrum, intra- and intermolecular cross peaks are observed and assigned (see text).

Table 1. Proton Chemical Shifts of the CHR-d(TTGGCCAA)$_2$ complex with Co(II)

Proton Chemical Shifts of d(TTGGCCAA)$_2$

	NH	$NH_{2(h-bond)}$	$NH_{2(ex)}$	H8	H2	H6	H5	H1′	H2′	H2″	H3′	H4′	H5′	H5″
T1						7.07	0.78	5.76	1.87	2.31	4.39	3.91	3.46	
T2						7.22	0.72	6.31	2.53	2.80	4.99	4.50	4.15	
G3	12.11	15.06	13.09	8.05				8.41	4.48	4.97	5.86	5.76	5.03	5.11
G4	−2.91	−26.86	18.44	7.54				11.89	8.23	11.50	6.23	8.53	5.79	6.17
C5		0.25	1.07			4.66	0.34		−29.45	−20.82	−0.48	28.54	11.19	15.96
C6		3.47	−0.26			−14.72	−6.22		−3.58		−7.37	−38.59	−18.35	−41.21
A7				6.32	8.04*			8.50	2.48	3.57	5.79	5.95	3.03	
A8				8.20	7.72*			6.95	2.79	3.04	5.48	5.60	5.77	6.40

Proton Chemical Shifts of Chromomycin-A_3 sugar residues

	H1	$H2_{ax}$	$H2_{eq}$	H3	H4	H5	H6	acetyl	other
A	18.13	10.49	10.64	9.77	9.90	11.20	7.48	6.46	
B	8.45	4.07	4.42	7.11	5.43	7.31	3.21		4.76(OCH_3)
C		23.18†		46.72†	5.96†		−3.84		
D	45.07	9.14	13.46	21.82	12.13	22.68	9.64		14.63(OH)
E	14.84	6.98	6.90	6.03	9.29	12.05	8.31	4.78	

Proton Chemical Shifts of Chromomycin-A_3 chromophore

	H2	H3	H4a	H4e	H5	H7	OH8	H10	H1′	H1′OMe	H3′	H4′	H5′
CHR	−59.28	−19.06	−8.82	−1.41	32.16	26.93		15.25	−11.45	−5.60	−3.21	−1.69	−3.16

*Determined from $^{13}C - {}^{1}H$ HMQC experiment; †tentative

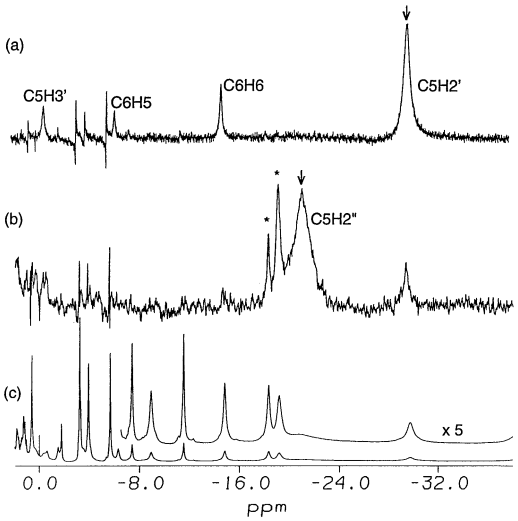

Figure 5. One dimensional NOE experiment indicating the assignment of protons of the C5 and C6 residues of the DNA. Peaks irradiated are indicated by ↓. (a) 200 ms irradiation of the C5H2′ proton with a 2500 Hz field produced NOE's at C6H6, C6H5 and C5H3′. (b) 100 ms irradiation of the C5H2″ proton with a 100 Hz field produced an NOE to C5H2′. (c) Upfield region of the spectrum of the Co(II) complex, for reference.

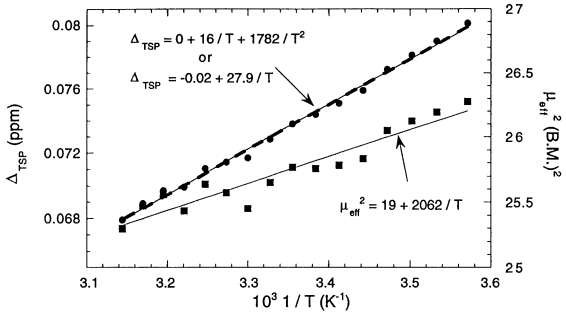

Figure 6. Plot of the paramagnetic component, $\Delta_{TSP,}$ of the isotropic shift of the internal reference TSP as a function of the inverse temperature. Δ_{TSP} is obtained as the difference between the TSP reference position in the Co(II) sample at various temperatures and the Zn(II) sample (invariant with temperature). Both a linear and quadratic fit to the data are shown in the figure (see text). The calculated effective dipole moment μ_{eff} is also plotted as a function of temperature, and a linear temperature dependence of μ_{eff}^2 is observed.

a 1.6 mM solution. The plot of Δ_{TSP} as a function of temperature in Figure 6 shows an apparent linear temperature dependence.

For cylindrical geometry, the measured shift is related to the molar paramagnetic susceptibility χ_M^P by the equation (Phillips and Poe, 1972):

$$\Delta_{TSP} = \frac{4\pi}{3}\frac{\chi_M^P}{V_M} = \frac{4\pi}{3V_M}\frac{N_A\mu_\beta{}^2}{3kT}\mu_{eff}{}^2 = \frac{0.84}{T}\mu_{eff}{}^2, \quad (3)$$

where V_M is the molar volume of the sample. This gives a molar susceptibility of $1.04 * 10^{-2}$ cm^3 mol^{-1} for the cobalt complex at 25 °C. The second half of Equation 3 relates the shift to the effective dipole moment μ_{eff} in Bohr magnetons. N_A is Avogadro's number, μ_B is the Bohr magneton, k is Boltzmann's constant and T is the temperature. A value of μ_{eff} = 5.0 BM is obtained, corresponding to an isotropic g value of 2.6 ±0.2. (g is clearly anisotropic, but its average value is defined here, assuming $S = 3/2$ and $g^2S(S+1) = \mu_{eff}{}^2$. This value is used in the analysis of relaxation below.) The error margin allows for the uncertainty in measuring the exact concentration of the complex.

Evidence for non-Curie behavior

In Figure 6, $\mu_{eff}{}^2$ (from Equation 3) is plotted as a function of temperature. It is not a constant, but decreases with increase in temperature. We may write

$$\mu_{eff}{}^2 = \mu_{eff}{}^2(0) + \frac{m}{T},$$

where $\mu_{eff}(0)$ is the value of μ_{eff} at $1/T$ = 0 K^{-1}. Hence

$$\Delta_{TSP} = \frac{a}{T} + \frac{b}{T^2}, \quad (4)$$

where $a = 0.84\mu_{eff}{}^2(0)$, $b = 0.84$ m.

The linear dependence of $\mu_{eff}{}^2$ on temperature confers a quadratic dependence on Δ_{TSP} (and χ_M^P) and results in non-Curie behavior of this system. Although Δ_{TSP} in Figure 6 can be fit with a linear curve, the slope predicts an apparent μ_{eff} of 5.77 BM which significantly exceeds the range of 4.92–5.01 BM determined between 7 and 45 °C. Instead, the fitting of Δ_{TSP} to a quadratic curve with an intercept of 0 at $T^{-1} = 0$ K^{-1} gives an equivalent fit to the observed data but takes the non-Curie behaviour into account. Values of a and b determined from Equation 4 are $a = 15.9 \pm 0.1$($\mu_{eff}(0) = 4.35$ BM.), $b = 1760 \pm 25$. The quadratic term contributes about 25% of the total observed susceptibility shift at 25 °C.

Susceptibility tensor

The full susceptibility tensor has been determined from the above measurement of the isotropic molar susceptibility χ_M^P, assuming transferability from molar to molecular susceptibility values, and from the determination of the anisotropic susceptibility tensor components $\Delta\chi_{ax}$ and $\Delta\chi_{rh}$ from Equation 2 (see Experimental Methods). Equation 2 assumes that the electrons can be treated as a point dipole at the metal (Golding and Stubbs 1979).

One hundred and thirty-eight measured pseudocontact shifts were used in a least squares fit of Equation 2. Chromophore protons and H1, H2 and H3 protons of the C sugar were excluded from the analysis because of unknown contact shift contributions. The coordinates used were from the refined NMR structure (Tu and Gochin, in preparation). The molecular reference frame is defined with the metal ion at the origin, the *z*-axis along the C2 axis of symmetry of the complex, and the *y*-axis in the plane of the two O1 oxygen atoms of the chromophores. The tensor obtained is $\Delta\chi_{ax} = 3.58 * 10^{-3}$ cm^3/mol, $\Delta\chi_{rh} = -6.06 * 10^{-4}$ cm^3/mol; $\alpha = 80(\pm 1)°$, $\beta = 90(\pm 1)°$, $\gamma = 0(\pm 1)°$ at 25 °C. Figure 7 shows the fit of observed and calculated data. Superimposed on the data in Figure 7 are the chromophore shifts which were not used in the calculation of the tensor, and which exhibit contact contributions to their total shift. The RMS deviation between observed and calculated shifts was 0.2 ppm over a shift range of ~100 ppm.

From the measured solution susceptibility, it is then possible to calculate the *x*, *y* and *z* components of the tensor as $\chi_{xx} = 8.9 * 10^{-3}$ cm^3/mol, $\chi_{yy} = 9.5 * 10^{-3}$ cm^3/mol, $\chi_{zz} = 12.8 * 10^{-3}$ cm^3/mol. The anisotropic susceptibility is similar in magnitude to that obtained for 5-coordinate Co(II) in carbonic anhydrase adducts (Banci et al., 1992) and larger than that of tetrahedral Co(II) in a zinc finger (Harper et al., 1993) . However, the larger rhombicity observed for Co(II) in carbonic anhydrase is not seen here; instead the tensor is almost axially symmetric, as was found for the zinc finger complex. Figure 8 depicts the tensor in the molecular framework. The principal axis of the tensor does not lie along the C2 axis of symmetry, but rather perpendicular to it in the direction of the O9 atoms.

Relaxation measurements

The electronic relaxation time τ_s was determined to be 1–4 ps from T_{1M} studies (Figure 9a). From a study of

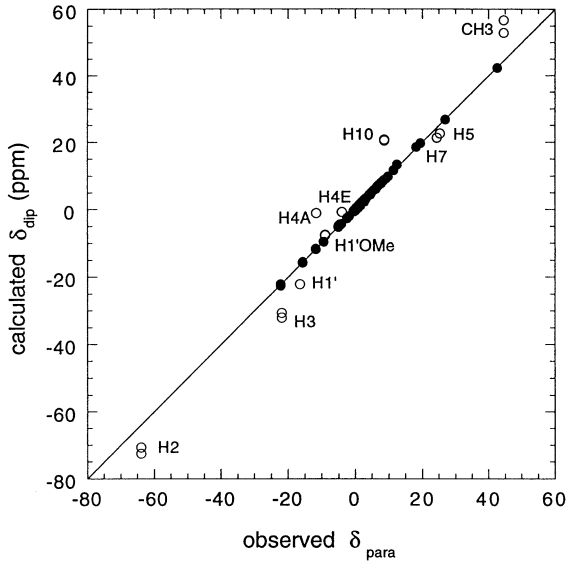

Figure 7. Plot of the observed paramagnetic shift versus calculated dipolar shift for 138 pseudocontact shifted protons (•). The calculated shifts were obtained from a fit of the susceptibility tensor anisotropy and orientation in Equation 2. Superimposed on the plot are the contact shifted chromophore protons (○) which were not used in the tensor refinement.

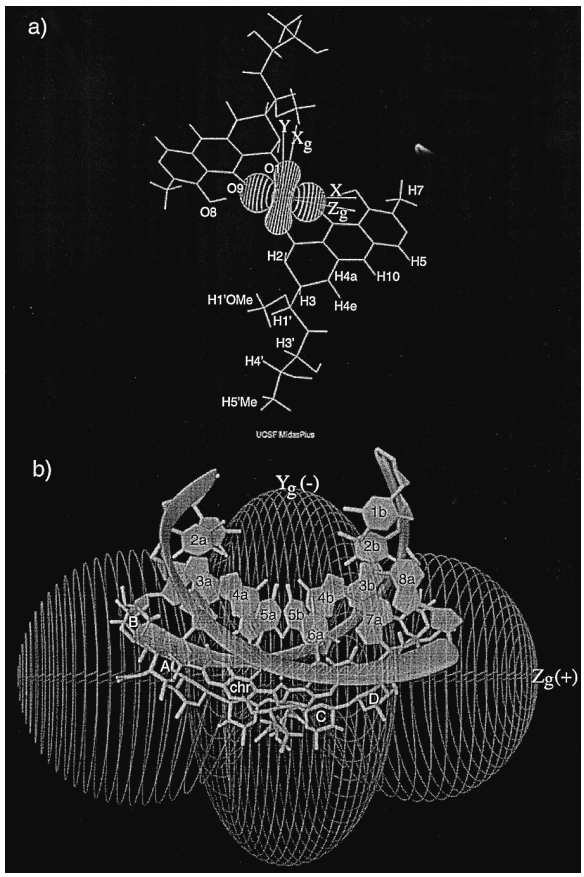

Figure 8. (a) Depiction of the coordination site of the Co(II) and four chromophore oxygen atoms. The molecule is drawn in the *XY* plane of the molecular reference frame, with *Z* coming out of the plane of the paper. The positive (Z_g) and negative(X_g) lobes of the susceptibility tensor anisotropy are indicated. Y_g(negative) is perpendicular to the paper. Note that Z_g and *Z* are perpendicular to each other. (b) The DNA-chromomycin-Co(II) complex superimposed on a ± 1ppm surface of the dipolar shift. This view is rotated by 90° about *X* with respect to (a).

linewidth changes between 500 MHz and 300 MHz, we extracted the Curie component of the linebroadening and obtained a value for the isotropic *g* tensor of 3.1 ± 0.3, assuming a rotational correlation time τ_r =4 ns, estimated from the size of the complex, and $\tau_s = 2$ ps. By doubling the rotational correlation time to 8 ns, a value of $g = 2.7$ is obtained. A comparison of observed and calculated paramagnetic line broadening in Figure 9b shows a fairly good correlation between observed values and those calculated using $\tau_r = 8$ ns, although there is scatter in the data. The apparent deviation of the data at distances greater than 10 Å in Figure 9b is mostly a result of the logarithmic *y*-scale, which magnifies discrepancies for protons that show only a small amount of broadening. It should not be taken as an indication of a breakdown in the r^{-6} relationship.

Discussion

Applicability of standard NMR methods to the paramagnetic case

The relative ease of assignment of the cobalt complex and the observation of all expected NOE cross-peaks indicates that the presence of high spin Co(II) does not preclude the use of standard NMR experiments for spectral analysis. This is primarily a result of the short electronic relaxation time of high spin Co(II), which prevents excessive line broadening of all but the closest protons (< 4 Å away). The principal component of the line broadening is Curie relaxation; hence spectra at lower field will have dramatically sharper resonances for protons within a 7 Å sphere of the metal. Since the Curie effect does not contribute to the T_1 relaxation, the NOEs remain strong and can be used for assignment and structural studies (Bertini et al., 1996b, 1997).

Similarly, relatively high quality DQFCOSY and TOCSY spectra were observed for this complex, with

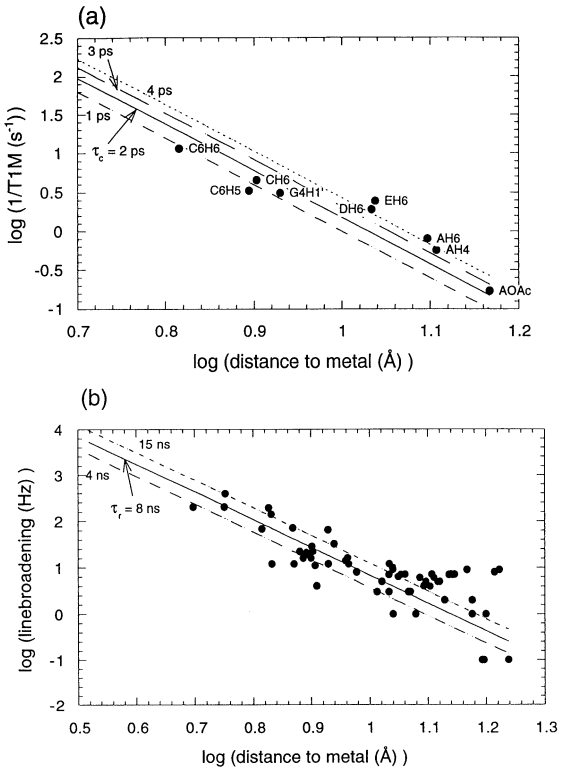

Figure 9. Paramagnetic relaxation rates of the DNA-drug complex as a function of distance from the metal. Paramagnetic relaxation was measured as the difference between the relaxation rates observed in the Co(II) and Zn(II) complexes. (a) Longitudinal paramagnetic relaxation($1/T_{1M}$): experimental (•), and calculated for molecular correlation times $\tau_c = 1$, 2, 3 and 4 ps. (b) Paramagnetic line broadening ($1/\pi T_{2M}$): experimental (•), and calculated for molecular rotational correlation times $\tau_r = 4$, 8 and 15 ns. Double log plots are shown.

about 60% of the expected cross-peaks actually observed. The remainder correspond to protons for which at least one member of the pair is < 10 Å from the Co(II). Some additional spurious cross-peaks are observed in the DQFCOSY, which do not correspond to pairs of J-coupled protons but are rather cross-correlation cross-peaks (Bertini et al., 1993; Qin et al., 1993). We observe three or four of these relaxation-allowed cross-peaks (Desvaux and Gochin, in preparation). However, they do not encumber the assignment procedure because very few of them are observed. They are limited by the requirement for lines narrow enough to be observed as doubly-antiphase cross-peaks, and for a proton–proton $-S$ spin geometry that is essentially linear. In addition these peaks are absent in TOCSY spectra which can be used to cross-check for validation. Therefore they are not of significant concern when applying COSY correlation maps to assignment procedures for paramagnetic molecules.

Geometry of the metal center

The values obtained for the magnetic susceptibility and electronic relaxation time indicate that the coordination geometry around the Co(II) is distorted octahedral. The UV absorption spectrum (not shown) correspondingly shows no absorption bands above 500 nm, which would be characteristic of the allowed d–d transitions in tetrahedral Co(II) complexes. Spin–orbit coupling makes a strong contribution to the effective magnetic moment, which for three (isolated) unpaired electrons would be 3.87 BM. Spin-orbit coupling changes the observed magnetic moment (Cotton and Wilkinson 1972):

$$\mu_{S+L} = \sqrt{4S(S+1) + L(L+1)}$$

where here $S = 3/2$ and $L = 3$, giving a total possible effective magnetic moment of 5.2. A value of 5.0 ± 0.4 is actually observed in this complex, corresponding to a partial quenching of the orbital angular momentum due to restricted motion of the electrons. The size of μ_{eff} is in accordance with values observed for octahedral complexes. Tetrahedral complexes give lower values of μ_{eff} due to significant quenching of orbital angular momentum. At high temperature, the effect of spin-orbit coupling can be neglected so that one should approach the free electron limit at $1/T = 0$. Indeed a value for g of 2.2, close to the free electron value, is obtained by extrapolation to $1/T = 0$.

Additionally, the short electronic correlation time τ_s is indicative of octahedral geometry. Efficient electronic relaxation occurs because of the existence of many low lying excited states in distorted octahedral complexes (Bertini and Luchinat, 1984). The geometry of the published NMR structure (Gao et al., 1992) shows four-coordinate metal ligation, and it is assumed that the fifth and sixth ligands are water molecules in rapid exchange. Indeed these are observed in the crystal structure of a similar complex (C. Ogata, X. Gao and W. Hendrickson, unpublished data).

Orientation of the susceptibility tensor

The orientation of the susceptibility tensor with respect to the ligand geometry is shown in Figure 8a. The positive lobes of the tensor Z_g extend in the direction of the two O9 coordinating ligands perpendicular to the C2 axis of symmetry. This is also the direction

of largest paramagnetic susceptibility, $\chi_{zz} = 1.28 * 10^{-2}$ cm^3/mol. Y_g, with $\chi_{yy} = 0.95 * 10^{-2}$ cm^3/mol, lies more or less along the direction of the metal – O1 bonds, and X_g, with $\chi_{xx} = 0.89 * 10^{-2}$ cm^3/mol, is along the C2 axis of symmetry. The ligand field is strongly distorted from an octahedron. Figure 8b shows the orientation of the tensor globally within the complex. The tensor induces strong downfield shifts of the A,B, D and E sugar protons, and strong upfield shifts of the protons of residues G4, part of C5, and C6 as well as those of the hydrophilic side chain attached to the chromophore. Residue C5 lies on both sides of the ± tensor boundary, with C5H4′ and C5H5′,H5″ being strongly downfield shifted, and C5H2′, H3′, H5 and H6 strongly upfield shifted. The position of this residue is therefore extremely precisely defined in the tensor frame. Or *vice versa*, the pseudocontact shifts of this residue precisely define the tensor orientation.

The DNA protons experience significant pseudocontact shifts for all eight base pairs. In terms of magnitude, the order of average shift size is C5 > C6 > G4 > G3 > A7 > A8 > T2 > T1. This has bearing on the precision with which these residues can be defined by the pseudocontact shift.

Sensitivity of pseudocontact shifts to structure

An example of the sensitivity of the pseudocontact shifts in defining long range structure of the DNA is given in Table 2. It illustrates the calculated ^{31}P pseudocontact shifts for three DNA forms, B, C and the somewhat distorted DNA that results from drug complexation. All three forms were superimposed at the G4 and C5 bases. B and C DNA differ by only 1.04 Å RMSD and have virtually identical calculated NOE data sets, but give substantially different ^{31}P pseudocontact shifts. The distortion due to the drug binding is readily observed from the shifts.

Electron distribution around the metal; factoring of the hyperfine shifts

An understanding of the electron distribution around the site of metal ligation and the extent of electron cloud dispersion can be obtained by examining the contact shifts of protons attached to the chromophore. Since the susceptibility tensor anisotropy is accurately known and the ligand-centered contribution to proton dipolar shifts can be considered negligible (Kurland and McGarvey, 1970) , we can factor the observed isotropic shifts into contact and dipolar contributions.

The results listed in Table 3 show that the isotropic shifts are primarily dipolar in origin and contact shifts are relatively small. The boundary between the negative and positive lobes of the susceptibility tensor passes very close to the chromophore H4A, H4E protons, which lie almost at the magic angle and therefore have a very small dipolar shift. H2, H3 and H1' chromophore protons show strong upfield isotropic shifts while H5, H10, HO8 and the H7 and C7 methyl positions are strongly downfield shifted. The uniformity in shift direction for a given group of protons is indicative of predominant geometric shift effects. The error margins in the calculated dipolar shifts were obtained by comparing shifts obtained in the previous published structure (Gao et al., 1992) as well as our refined structure (Tu and Gochin, in preparation).

Contact shifts are indicative of the electron spin delocalization and the type of molecular orbitals containing the unpaired spin(s) (La Mar et al., 1973). Some evidence of σ spin delocalization exists in the observation of relative contact shifts in the order H3 ≥ H2 > H1′ > H1′Me = H3′ = H4′ = H5′ = 0. Shifts are upfield, implying a negative spin-density, possibly through π → σ spin polarization (La Mar et al., 1973; Goff, 1981). π-type molecular orbitals may play a role in the unpaired electron spin delocalization around the conjugated rings. Nevertheless, spin density is not transmitted more extensively through the π-conjugated rings. This is indicated, for example, by the small contact shift contribution at H5, which is comparable with that at H1′, or the lack of a contact shift contribution at AH1. The contact shift attenuates after ∼6 bonds from the metal, similar to the result seen with ferric complexes. The contact shifts are subject to revision upon further structure refinement because of the overwhelming geometric dipolar shift contribution.

Relaxation effects

The total observed longitudinal paramagnetic relaxation T_{1M} is also reported in Table 3. The dipolar longitudinal paramagnetic relaxation, T_{1M}^{dip}, is calculated from the known distance from each proton to the metal using the Solomon equation. Also shown in Table 3 are the data for CH6 and G4H1′, which are not in the immediate sphere of ligation and are not subject to contact shifts. It appears that the isotropic equations for relaxation are not able to predict the measured values consistently (discrepancies are shown in italics in Table 3). An overall correlation between the observed

Table 2. ^{31}P pseudocontact shifts (ppm) in DNA octamers having Co(II) at the center

Phosphate	B-DNA[a]	C-DNA[a]	drug complex[b]	experimental
P(T1-T2)	−0.67	−0.69	−0.34	−0.22
P(T2-G3)	−0.52	−0.64	0.19	0.34
P(G3-G4)	0.29	0.03	1.63	1.43
P(G4-C5)	2.19	1.61	2.84	2.96
P(C5-C6)	−11.77	−13.85	−9.64	−9.46
P(C6-A7)	1.67	4.85	−4.34	−4.15
P(A7-A8)	8.13	10.34	1.29	1.37

[a] Simulated using Sybyl (Tripos Associates);
[b] from ref 23.

and calculated T_{1M} values exists (Figure 9a), but there is a large amount of scatter in the data, so that individual relaxation times cannot be reliably used to specify distance from the metal with high accuracy. Even larger scatter is observed in the T_{2M} data of Figure 9b. The Solomon equations are subject to the limitations of assuming that the unpaired electrons exist as a point dipole, g is isotropic and that a single correlation time (2 ps) describes the electronic relaxation. Calculation of paramagnetic relaxation rates relies on the assumption that the effect of zero field splitting and g anisotropy is reflected simply in a change of the constant defining the correspondence between T_1 or T_2 and r^{-6} (Bertini et al., 1997) . These factors clearly play an important role in the relaxation. Experimental errors also arise in both assumption of mono-exponential decay curves and in determination of T_{1M} and T_{2M} from the difference of two error-prone numbers.

Another indication of the inadequacy of the isotropic relaxation equations or the parameters used is observed in the computation of g using Curie relaxation. An apparent g value of 2.6 was obtained from susceptibility studies, and of 3.1 from Curie relaxation effects using a 4 ns rotational correlation time. However, the maximum value of the effective magnetic moment of 5.2 corresponds to a g value of 2.7. It is likely that the relaxation equations for isotropic g do not suffice to describe the relaxation of this complex. Alternatively, a larger rotational correlation time of 8 ns must be invoked to describe the Curie relaxation effects.

Conclusion

The NMR spectra of the complex formed between the drug chromomycin-A_3, a DNA octamer d(TTGGCCAA)$_2$ and high spin cobalt (II) have revealed that a strongly bound rapidly relaxing paramagnetic metal complex exists, with narrow lines for most resonances and good quality spectra. An electronic relaxation time τ_s of 1–4 ps has been determined. Since it is so short it dominates the molecular correlation time and $\tau_c = \tau_s$. The spectra were assigned by traditional NMR methods. Large hyperfine shifts occur, of which the principal components are the isotropic dipolar shifts. These properties are typical of high spin cobalt found in other complexes. The excellent agreement obtained between observed pseudocontact shifts and calculated dipolar shifts demonstrates that the dipolar Equation 2 adequately describes the pseudocontact shift, even for the protons less than 7 Å from the metal, and therefore that the electrons can be considered to act as a point dipole for shift calculation purposes. Contact shifts and hyperfine coupling constants appear to be small compared to values obtained in iron complexes (Satterlee and La Mar, 1975; Goff and La Mar, 1977; Wu and Kurtz, 1989; Banci et al., 1995) for the directly coordinated groups. This would imply that electron delocalization around the chromophore ring is not extensive, with the electrons residing to a large extent at the metal center.

Protons 6 Å or more from the cobalt ion can be readily observed, and, in several cases, closer protons have also been found and assigned; for example the C5H2″ proton in Figure 5. T_1 relaxation is dipolar in origin and T_2 relaxation is probably 90% Curie and 10% dipolar at 500 MHz and 25 °C. A tentative rotational correlation time of 8 ns is obtained from this study. Proton linewidths and T_1 measurements

Table 3. Isotropic shifts and relaxation rates for chromomycin chromophore protons

	δ_{para} (ppm)	δ_{dip} (ppm)	δ_{con} (ppm)	$T_{1M}{}^{-1}$ (s^{-1})	$T_{1M}{}^{-1}$ $dip_{(}s^{-1})$[a]	$T_{1M}{}^{-1}$ $con_{(}s^{-1})$	$r_{M(II)}$ (Å)	bonds from M(II)
Protons directly on chromophore								
Non-conjugated ring								
H2	−63.9	−69.7±5.4	5.8±5.4	20				3
H3	−21.9	−30.9±0.7	9.0±0.7	20	*54*		5.5	4
H4A	−11.5	0.3±1.7	−11.8±1.7	16	*46*		5.6	5
H4E	−4.3	0.8±1.3	−5.1±1.3	12	*19*		6.5	5
Conjugated ring								
H5	25.2	21.3±0.6	3.9±0.6	9.5	6	3.5	7.9	5
H10	8.5	20.9±0.5	−12.4±0.5	14	*14*		6.8	5
Substituents on chromophore								
Non-conjugated ring								
H1′	−16.5	−21.2±0.7	4.7±0.7	6	*17*		6.6	6
H1′Me	−9.1	−8.2±2.7	−0.9±2.7	2.2	3.0	∼0	8.6	7
Conjugated ring								
AH1	12.5	12.8±0.5	−0.3±0.5	2.5	2.5	0	9.1	7
H7Me	24.2	19.4±1.1	4.8±1.1	13.8	7.6	6.2	7.6	6
C7Me	23.9	23.3±1.5	0.6±1.5†					5
Other								
CH6	−5.1	−5.3±0.6	0.2±0.6	5.3	5.4	0	8.0	9
G4H1′	−6.2	−5.8±0.6	−0.4±0.6	3.2	3.7	∼0	9.4	–

[a] $1/T_{1M}{}^{dip}$ calculated using Solomon equation with $g = 2.6$ and $\tau_c = 2$ ps.
† Includes a possible ligand-centered shift

have not accurately reflected distances from the metal center, especially for close protons. This is possibly due to the limitations of using the isotropic Solomon equations to describe the relaxation. It may also be associated with errors in measuring the relaxation rates. It is however also possible that the geometry in the immediate vicinity of metal ligation needs to be adjusted to accommodate a more octahedral-like coordination sphere. This will be the subject of a future study.

The three unpaired electrons at the cobalt exhibit decidedly non-Curie behavior, both in macroscopic measurements of solution susceptibility and microscopic measurements of individual proton shifts as a function of temperature. This is a reflection of the sizable zero field splitting at the cobalt. Consequently a value for the electronic g of 2.6 ± 0.2 is obtained.

The orientation and magnitude of the magnetic susceptibility tensor has been determined in this study. The tensor is nearly axially symmetric with the positive lobes (z axis) at 90° from the molecular C2-axis of symmetry, and in the direction of the O9 ligands which coordinate the metal to the conjugated ring system of the chromophore. The susceptibility anisotropy is large; $\chi_{ax} = 3.58 * 10^{-3}$ cm^3/mol and $\chi_{rh} = -0.61 * 10^{-3}$ cm^3/mol; in terms of shifts in ppm, the corresponding values are $\chi_{ax} = 5940$ ppm Å^3 and $\chi_{rh} = -1006$ ppm Å^3. Therefore the paramagnetic shifts can provide valuable long-range structural information on the residues surrounding the metal to a distance of up to 30 Å, and down to ∼ 5 Å. A nucleus at 30 Å along the axial direction of the tensor would experience a dipolar shift of 0.2 ppm. At the same time, care must be exercised when attempting to use relaxation rates to correlate distances from the cobalt(II).

Acknowledgements

This work was supported by National Institutes of Health grant GM53164. We acknowledge use of the Computer Graphics Laboratory at UCSF, supported by NIH P41-RR01081. The author is grateful to P.V. Scaria for help in determining the extinction coefficient of the DNA octamer, and to V.J. Basus for critical reading of this manuscript. Supplemental Material:

Figures showing the ID NOE assignment of chromophore protons, and tables of ^{31}P chemical shifts, and IH chemical shifts in the Zn complex, are available from the author upon request.

References

Banci, L., Dugad, L.B., La Mar, G.N., Keating, K. A., Luchinat, C. and Pierattelli, R. (1992) *Biophys. J.*, **63**, 530–43.

Banci, L., Bertini, I. Pierattelli, R., Tien, M. and Vila, A (1995) *J. Am. Chem. Soc.*, **117**, 8659–8667.

Banci, L., Bertini, I., Gray, H., Luchinat, C., Reddig, T., Rosato, A. and Turano, P. (1997a) *Biochemistry*, **36**, 9867–77.

Banci, L., Bertini, I, Savellini, G.G., Romagnoli, A., Turano, P., Cremonini, M.A., Luchinat, C. and Gray, H.B. (1997b). *Proteins Struct. Funct. Genet.*, **29**, 68–76.

Banville, D.L., Keniry, M.A., Kam, M. and Shafer, R.H. (1990) *Biochemistry*, **29**, 6521–34.

Bertini, I. and Luchinat, C. (1984). *Adv. Inorg. Biochem.*, **6**, 71–111.

Bertini, I. and Luchinat, C. (1986) In *NMR of Paramagnetic Molecules in Biological Systems*, Benjamin/Cummings.

Bertini, I., Luchinat, C. and Tarchi, D. (1993) *Chem. Phys. Lett.*, **203**, 445–449.

Bertini, I., Jonsson, B., Luchinat, C., Pierattelli, R. and Vila, A. (1994) *J. Magn. Reson. Ser. B*, **104**, 230–239.

Bertini, I., Luchinat, C. and Rosato, A. (1996) *Prog. Biophys. Mol. Biol.*, **66**, 43–80.

Bertini, I., Donaire, A., Felli, I. and Rosato, A. (1996) *Magn. Reson. Chem.*, **34**, 948–50

Bertini, I., Donaire, A., Luchinat, C. and Rosato, A. (1997) *Proteins*, **29**, 348–58.

Brown, S., Weber, P. and Müller, L. (1988) *J. Magn. Reson.*, **77**, 166.

Cheng, H. and Markley, J. (1995) *Annu. Rev. Biophys. Biomol. Struct.*, **24**, 209–237.

Cotton, F. and Wilkinson, G. (1972) In *Advanced Inorganic Chemistry*, John Wiley and Sons, Inc.

Day, M. (1994) STRIKER. University of California, San Francisco.

Desvaux, H. and Gochin, M., in preparation.

Emerson, S. D. and La Mar, G.N. (1990) *Biochemistry*, **29**, 1556–66.

Ferrin, T., Huang, C., Jarvis, L. and Langridge, R. (1988). *J. Mol. Graphics* **6**, 13–27.

Gao, X. and Patel, D.J. (1989) *Biochemistry*, **28**, 751–762.

Gao, X. L. and Patel, D.J. (1990) *Biochemistry* **29**, 10940–10956.

Gao, X. L., Mirau, P. and Patel, D.J. (1992) *J. Mol. Biol.*, **223**, 259–79.

Gochin, M. and Roder, H (1995) *Protein Sci.*, **4**, 296–305.

Gochin, M. (1997) *J. Am. Chem. Soc.*, **119**, 3377–3378.

Goddard, T. and Kneller, D. (1997) SPARKY. University of California, San Francisco,

Goff, H. and La Mar, G.N. (1977) *J. Am. Chem. Soc.*, **99**, 6599–6606.

Goff, H. (1981) *J. Am. Chem. Soc.*, **103**, 3714–3722.

Golding, R. and Stubbs, L. (1979) *J. Magn. Reson.*, **33**, 627–647.

Griswold, B., Humoller, F. and McIntyre, A. (1951) *Anal. Chem.*, **23**, 192–194.

Harper, L. V., Amann, B. T., Kilfoil Vinson, V. and Berg, J. M. (1993) *J. Am. Chem. Soc.*, **115**, 2577–2580.

Kurland, R. and McGarvey, B. (1970) *J. Magn. Reson.* **2**, 286–301.

La Mar, G.N., Horrocks Jr., W. and Holm, R. (1973) In *NMR of Paramagnetic Molecules: Principles and Applications*, Academic Press.

Levitt, M., Frenkiel, T. and Freeman, R. (1982) *J. Magn. Reson.*, **47**, 328.

Marion, D. (1994) *Biochimie*, **76**, 631–640.

Phillips, W. and Poe, M. (1972) *Methods Enzymol.*, **24**, 304–311.

Piotto, M., Saudek, V. and Sklenar, V.J. (1992) *J. Biomol. NMR*, **2**, 661.

Press, W., Teukolsky, S., Vetterling, W. and Flannary, B. (1992) *Numerical Recipes in Fortran; The Art of Scientific Computing* Cambridge University Press.

Qin, J., Delaglio, F., La Mar, G.N. and Bax, A. (1993) *J. Magn. Reson., Ser. B*, **102**, 332–336.

Renault, J., Verchere–Beaur, C., Morgenstern-Badarau, I. and Piccioli, M. (1997) *FEBS Lett.*, **401**, 15–19.

Salgueiro, C., Turner, D. and Xavier, A. (1997) *Eur. J. Biochem.*, **244**, 721–734.

Satterlee, J. and La Mar, G.N. (1975) *J. Am. Chem. Soc.*, **98**, 2804–2808.

Sette, M., Paci, M., Desideri, A. and Rotilio, G. (1993) *Eur. J. Biochem.* **213**, 391–397.

Sklenar, V., Miyashiro, H., Zon, G., Miles, H. and Bax, A. (1986) *FEBS Lett.*, **208**, 94–98.

Tu, K. and Gochin, M., in preparation.

Vila, A. and Fernandez, C. (1996) *J. Am. Chem. Soc.* **118**, 7291–7998.

Wimperes, S. and Bodenhausen, G. (1989) *Mol. Phys.*, **66**, 897.

Wu, F. and Kurtz, D. (1989) *J. Am. Chem. Soc.*, **111**, 6563–6572.